Article

Not peer-reviewed version

Sustainable Bioplastic Development from Shellfish Waste of Crab (Callinectes pallidus) and Periwinkle (Thais coronata) for Circular Applications in the Blue Economy

Isa Elegbede *, Opeyemi Avoseh, Hassan Shoyiga *, Jimoh Abayomi, Abdullai Ayomide, Nobathembu Faleni, Appolinaire Goussanou, James Sedie, Mutmainnat Adedamola

Posted Date: 18 March 2026

doi: 10.20944/preprints202603.1425.v1

Keywords: bioplastics; chitosan; periwinkle; crab; DFT; marine biopolymers; blue economy; circular bioeconomy; sustainability

 doi:10.20944/preprints202603.1425.v1

Article

Sustainable Bioplastic Development from Shellfish Waste of Crab (Callinectes pallidus) and Periwinkle (Thais coronata) for Circular Applications in the Blue Economy

Isa Elegbede [1,*], Opeyemi Avoseh [2], Hassan Shoyiga [3,*], Jimoh Abayomi [1], Abdullai Ayomide [1], Nobathembu Faleni [3], Appolinaire Goussanou [4], James Sedie [1] and Mutmainnat Adedamola [1]

[1] Department of Fisheries, Faculty of Science, Lagos State University, Ojo Campus, Lagos, Nigeria

[2] Department of Chemistry, Faculty of Science, Lagos State University, Ojo Campus, Lagos, Nigeria

[3] Faculty of Natural Sciences, Department of Applied Science, Walter Sisulu University, Old King William Town Road, Potsdam Site, East London 5200, South Africa

[4] University of Abomey-Calavi, Abomey-Calavi, Benin Republic

* Correspondence: hshoyiga@wsu.ac.za (H.O.); isaelegbede@gmail.com (I.O.)

Abstract

Shellfish waste from fisheries remains an underutilised yet valuable resource for advancing circular material innovation, particularly within the blue economy. This study presents the synthesis, characterisation, and theoretical evaluation of chitosan derived from the shells of crab (Callinectes pallidus) and periwinkle (Thais coronata) for bioplastic production. Chitosan was extracted using conventional deproteinization, demineralisation, and deacetylation techniques, then blended with starch and glycerol to produce biodegradable polymer films moulded for bioplastic product. Experimental characterisation using FTIR, SEM, EDS, and XRD confirmed the successful isolation and chemical integrity of chitosan. The chitosan from periwinkle showed increased levels of carbon and oxygen, indicating its improved yield and performance. Density Functional Theory (DFT) computations at the B3LYP/6-311G(d,p) level provided molecular insights on a two-unit chitosan model, revealing a HOMO-LUMO energy gap of -0.251 eV, indicating significant kinetic stability. The electrostatic potential (ESP) map showed electron-rich regions at -OH and -NH_2 groups, aligning with the experimentally observed adsorption potential. Additional quantum chemical descriptors, such as electrophilicity index, softness, and dipole moment, supported the high reactivity and structural flexibility of chitosan for polymer interaction. Theoretical FTIR vibrational analysis validated the chemical structure. The bioplastic product derived from periwinkle exhibited improved shape and elemental distribution, confirming its suitability for scalable biopolymer production. The combination of experimental results and computational modelling highlights the potential of marine-derived chitosan as an economical and sustainable alternative to petrochemical plastics, reducing carbon emissions and non-biodegradable waste.

Keywords: bioplastics; chitosan; periwinkle; crab; DFT; marine biopolymers; blue economy; circular bioeconomy; sustainability

1. Introduction

Plastic pollution is one of the trending environmental issues owing to the global increasing population. This material, generated from domestic or industrial use, reaches the shorelines to the depth of the ocean and continue to accumulate, threatening the aquatic environment and human health. Despite different awareness and policies, the demand for plastics continues to rise, caused by cumulative domestic and industrial needs. Thus, there is a continuous interest in exploring safer,

 doi:10.20944/preprints202603.1425.v1

more sustainable alternatives that meet the organic demand of humans with minimal detrimental effect on the environment. One of the best solutions is the development of bioplastics from renewable sources for easy biodegradation. Yet, while commercial chitosan production often relies on shrimp and lobster shells, other shellfish species remain largely untapped, particularly in regions like West Africa.

In coastal regions, shellfish like the crab (Callinectes pallidus) and periwinkle (Thais coronata) are widely consumed. Their shells, however, are typically discarded as waste, contributing to environmental and public health challenges. At the same time, these shells are rich in chitin, a key precursor to chitosan, which presents an opportunity for value addition and waste recovery. Unfortunately, there is limited research on the biochemical properties, processing potential, and performance of chitosan derived from these species.

This gap matters. Using local shellfish waste to develop bioplastics could help reduce environmental waste, create new economic opportunities, and support Nigeria's transition to a circular economy. Moreover, when framed within the blue economy, this approach emphasises the sustainable use of marine resources for inclusive development, aligning environmental goals with livelihood improvement.

Currently, it is difficult to conceive of a society devoid of plastics or synthetic organic polymers, despite their extensive production and utilisation commencing since the 1950s. Despite the emergence of the first synthetic plastics, such as Bakelite, in the early 20th century, widespread utilisation of plastics in nonmilitary applications did not occur until the end of World War II [1]. Since that time, plastic output has surged dramatically, surpassing that of most other synthetic materials. Plastic production has risen annually over the past 15 years, with an anticipated worldwide output of 299 million tonnes in 2013. Packaging can be constructed from several materials, including metals, glass, wood, paper or pulp, polymers, or composites, which are combinations of multiple elements [2]. Plastic polymers are utilised not just for consumer products but also for the production of synthetic fibres, foams, coatings, adhesives, and sealants, which are employed in many applications. Plastics are an essential component of all aspects of modern life. Its versatility, dimensions, lightweight nature, and cost-effectiveness render it an exceptionally attractive material for diverse residential and industrial applications [3]. Given that plastics are utilised in many aspects of life, most polymers are derived from oil (i.e., hydrocarbons) and are produced by addition or condensation polymerisation methods. Many are believed to impact the ecosystem due to their prolonged biodegradation period. In 2007, the consumption of oil-based plastic reached 260 million tonnes. This constitutes a significant issue, as oil reserves are projected to diminish swiftly within the next 30 years [4]. Despite the widespread practice of polymer recycling and collection, a minimal amount gets transformed into new products. The majority is incinerated to harness energy [5].

Regrettably, excessive use and negligence of plastic harm the environment and threaten human health. The detrimental environmental impacts of petrochemical-derived plastic products are increasingly recognised [6]. Due to the toxicity and environmental ramifications of plastic additives, the proper breakdown or treatment of these compounds is crucial [7]. Various motivations compel corporations and researchers to pursue alternatives to non-renewable resources; however, it is essential to highlight that all prospective substitutes for existing plastics must satisfy certain critical criteria: they must be cost-effective, renewable, sustainable, and biodegradable [8]. Biodegradable bioplastics are designed for single-use, ephemeral applications. Biomass-derived durable polymers will supplant conventionally produced plastic items. Bioplastics can reduce carbon dioxide emissions by 30-70% compared to standard plastics [9]. Bioplastics are progressively utilised as a sustainable energy source [10].

Numerous studies have been conducted to address plastic waste on Earth by identifying environmentally superior alternatives to plastics. Microorganisms' enzymatic activity may efficiently decompose bioplastics, an eco-friendly alternative that can be disposed of in the environment. Bioplastics typically exhibit a diminished environmental impact compared to

 doi:10.20944/preprints202603.1425.v1

conventional plastics, as demonstrated by their lower carbon footprint and improved biodegradability, leading to a reduction in plastic waste [11]. Green chemistry, or sustainable chemistry, involves the design of chemical products and processes that limit or eliminate the use of compounds detrimental to humans, animals, plants, and the environment. Consequently, expenses must be minimised and energy efficiency maximised. A polymer that complies with the principles of green chemistry is termed a "green polymer" [12]. Consequently, bioplastics may be designated as green polymers. Aimikhe and Lekia et al. [13] assert that the waste produced by the periwinkle (Tympanotonus fuscatus) shell is significant. Periwinkle serves as a significant source of proteins and essential minerals in various culinary dishes within coastal cultures around. The shells of these aquatic species, recognised for their nutrient content, including calcium carbonate and chitin, contribute to environmental deterioration due to indiscriminate dumping. Kusumaningrum et al. [14] examined the use of biodegradable plastic goods made from nata de coco waste, which consists of roughly 42.57% cellulose, in conjunction with prawn shells that have a chitin level between 15-20%. Zhan et al. [15] performed a comprehensive review analysing the chemical structure, properties, and extraction methods of biopolymers derived from seafood waste, along with their applications in the packaging industry as reinforcement or foundational materials, intended to direct researchers towards viable alternatives to traditional plastics and promote their commercialisation. Chitin is a notable structural polysaccharide seen in invertebrates. For example, it is found in the exoskeleton of crustaceans, such as prawns, crabs, and periwinkles. Crab is a decapod crustacean. Approximately 4,500 species of crabs exist, exhibiting a wide variety of sizes and hues. Crustacean shell waste comprises approximately 30-40% protein, 30-50% calcium carbonate, and 20-30% chitin. These ratios fluctuate based on species and seasonal variations. Chitin and its derivative, chitosan, function as moisturising agents. The utilisation of crab shells can result in a reduction of marine waste management. Owing to its antibacterial qualities, extracted chitosan is extensively utilised in the food sector as a preservative [16]. Chitosan is mostly derived from the exoskeletons of crustacean shells, which are considered food waste. It is a linear polysaccharide composed of (1,4)-linked 2-amino-deoxy-β-D-glucan, and a deacetylated derivative of chitin, which ranks as the second most prevalent polysaccharide in nature, following cellulose. Chitosan is established as nontoxic, biodegradable, biofunctional, and biocompatible, and has antibacterial properties [17]. Chitosan is used in diverse sectors like pharmaceuticals, food, health, agriculture, and textiles. Additionally, it serves as a coagulant in wastewater treatment, moisturiser in facial creams, seed coatings, metal ion adsorbents, anti-cancer and anti-tumor agents, blood cholesterol regulators, supplementary components in animal feed, biopesticides, contact lenses, plaque inhibitors for teeth, accelerators for wound and bone healing, fat solvents, food preservatives, stabilisers, and colourants [18]. These characteristics render chitosan a highly appealing biomaterial. Owing to its bio-preservation effectiveness against food-borne infections, it may serve as a biodegradable and bio-preservative packaging material for food wrap and additional items.

This study investigates extraction techniques aimed at optimising the yield of pure biopolymer components, specifically chitosan (Ch) derived from crab and periwinkle shells, for the development of a biocompatible and eco-friendly bioplastic. The extracted chitosan was characterised using standard spectroscopic and analytical techniques, including SEM-EDX, FTIR, and XRD, to investigate its physicochemical properties and potential as an adsorbent for various applications. Furthermore, we introduced Ab initio quantum mechanical techniques to clarify the mechanistic properties of Ch, which were employed to validate our experimental approach. The Ch structure was modelled and optimised using density functional theory (DFT) calculations at the B3LYP level, which incorporates Becke's 3-parameter exchange functional and Lee Yang-Parr correlation energy [19,20], utilising the 6-311G (d, p) basis set. Subsequently, vibrational spectroscopy and theoretical optoelectronic properties were analysed using the TD-DFT technique. The highest occupied molecular orbital (HOMO) and the lowest unoccupied molecular orbital (LUMO) energies (ε) were evaluated, along with the conceptual-DFT indices of chemical potential (μ), hardness (η), softness (S), and electrophilicity (ω) based on the formulas proposed by Janak and Parr et al. [21] Additionally,

 doi:10.20944/preprints202603.1425.v1

electrostatic potential (ESP) and contour mapping were employed to elucidate the electronic and interatomic interactions of the molecule and their implications for adsorption properties.

2. Materials and Methods

2.1. Materials

Crab (*Callinectes pallidus*) and periwinkle (*Thais coronata*) shells were collected from local fish markets in the Ojo area of Lagos State. The materials used included sodium hydroxide, hydrochloric acid, a pH meter, sodium hypochlorite, and distilled water (DW).

2.2. Experimental

2.2.1. Preparation of Seafood Waste

The viscera and tissues of the crab and periwinkle were meticulously extracted and subjected to a hot air oven at 60 °C for 24 hrs, while the shells were cleaned and sun-dried at the LASU fish farm. The dried shell samples were subsequently ground using a dry grinder, yielding a powdered sample. Following the acquisition of shell powders, an attempt was made to extract chitosan from the shells. The powder was packed, sealed in an airtight plastic container, and stored in a cool, dry location.

2.2.2. Extraction Processes

The extraction of chitosan from crab and periwinkle shells comprises three main steps: deproteinisation, demineralisation, and deacetylation. The methods of deproteinisation, demineralisation, decoloration, dewatering, and deacetylation were utilised to extract chitosan and chitin from shell waste.

2.2.2.1. Extraction of Chitosan and Chitin from Crab Shells

i. Deproteinisation: The sample underwent deproteinisation using 300 ml of 1N NaOH at 90 °C for 24 hrs with continuous agitation. Fresh NaOH was added multiple times, and the sample was rinsed with distilled water each time before the addition of new NaOH. The sample was decanted after 24 hrs. The filtrate was rinsed with distilled water and subsequently dried. The weight was subsequently recorded [16].

ii. Demineralisation: The deproteinised crab shells underwent demineralisation using a 2.5% (w/v) hydrochloric acid solution at ambient temperature for 8 hours, aiming to eliminate the mineral content with a shell-to-solution ratio of 1:20 (w/v). The samples were filtered and rinsed for one hour with tap water until the pH reached neutrality. The demineralised shells were subsequently dried in the oven for 24 hrs.

iii. Decolouration and Dewatering: The sample underwent decolouration by being treated with acetone at a ratio of 1:10 for 10 mins, followed by drying for 2 hrs at ambient temperature. Utilise bleach containing 0.315% sodium hypochlorite for 5 mins at a ratio of 1:10 as previously indicated.

iv. Deacetylation: The chitin was subjected to treatment with 50% aqueous NaOH at a chitin to solution ratio of 15:1 (w/v) for 4 hrs. Subsequently, the chitin was filtered and rinsed with distilled water until the pH reached neutrality to yield chitosan [22]. The chitosan was subsequently dried for 24 hrs. The product was packaged as chitosan.

2.2.2.2. Extraction of chitosan and chitin from periwinkle shells

i. Deproteinization: The periwinkle shell (*Thais coronata*) waste was treated with a 4.0% NaOH solution with a ratio of ground shell to the solution of 1:20 (w/v) with constant stirring for 2h at 90 °C to remove the protein. The shell particles were then filtered, and the filtrates were washed with distilled water until the pH became neutral [22].

 doi:10.20944/preprints202603.1425.v1

ii. Demineralisation: Demineralisation was carried out at room temperature (32 ℃) by soaking 200g of ground samples in 1.5M HCl, until the evolution of gaseous effluent ceased. The demineralised samples were washed with distilled water to neutral, filtered and dried in the oven at 80 ℃ for 24hrs to constant weight [23].

iii. Depigmentation: Depigmentation and bleaching were carried out by soaking extracted chitin in 1M for 24hrs at 32 ℃. The chitin was then washed in distilled water and dried for 24hrs in an oven before characterisation [23].

iv. Deacetylation: The chitin obtained was treated with 50% aqueous NaOH with a ratio of chitin to the solution of 15:1 (w/v) for 4hrs. Then, the chitin was filtered and washed with distilled water until the pH became neutral to obtain the chitosan [22]. The chitosan obtained was then dried for 24hrs. The product was packed as chitosan. Figure 1 illustrates the aquatic waste materials used as starting materials for chitosan preparation and the obtained products at each preparation stage.

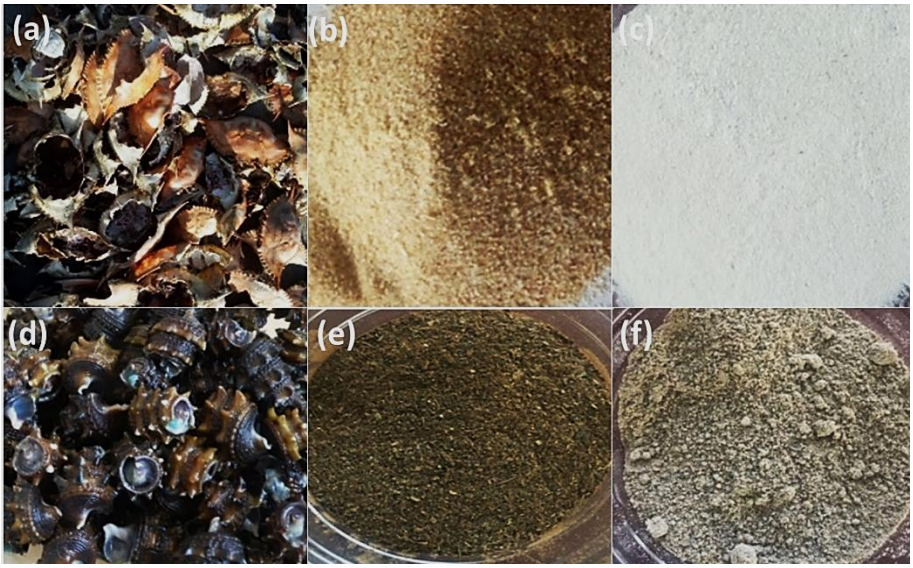

Figure 1. (a) Crab shells (*Callinectes pallidus*), (b) blended Crab shells, (c) crab powder after deacetylation, (d) Periwinkle shell (*Thais coronata),* (e) blended Periwinkle shell Periwinkle and (f) powder after Deacetylation.

2.3. Characterisation of Extracted Chitosan

2.3.1. Instrumentation

The chitosan samples obtained were characterised using several standard spectroscopic and microscopic methods. X-ray diffraction (XRD) patterns were obtained utilising Cu-Kα radiation (λ = 0.1540 nm) in a Rontgen PW3040/60 X'Pert Pro X-ray diffractometer, within the 2θ range of 10°–90° at a scan rate of 2° min^{-1}. Fourier transform infrared spectroscopy (FTIR) utilising a PerkinElmer 3000 MX spectrometer was employed to identify the functional groups in the materials throughout a wavelength range of 400-4000 cm^{-1}. The FTIR data were processed utilising Win-IR Pro Version 3.0 spectroscopy software. The scanning electron microscope (Quanta FEG 250, ThermoFisher Scientific, USA), fitted with an energy-dispersive X-ray spectroscopy (EDS) detector, was employed to examine the surface morphology and composition of the material at 15 kV.

2.3.2. Theoretical Studies

All electronic computations were conducted utilising Gaussian 09 software and the B3LYP functional. The Pople split-valence double-zeta 6-311 + g(d,p) [24] basis set was employed in all calculations. Numerous functionals with varying capacities have been developed and utilised by researchers across diverse disciplines. The B3LYP functional is classified as a hybrid exchange-correlation functional. It is formulated by integrating the Becke 8841 exchange functional with the

 doi:10.20944/preprints202603.1425.v1

LYP correlation functional, in conjunction with the local density approximation for the correlation functional. B3LYP is one of the most commonly utilised functionals in chemistry for the examination of standard chemical compounds. Subsequently, the energies of the highest occupied molecular orbital (HOMO) and the lowest unoccupied molecular orbital (LUMO) (ε) were utilised to calculate the conceptual-DFT indices of chemical potential (μ), hardness (η), softness (S), and electrophilicity (ω), employing the formulas established by Janak and Parr et al. [25]. These conceptual DFT indices have been extensively utilised in the literature and can be computed using equations 1-4.

$$\mu = \left(\frac{\partial E}{\partial N}\right)_{\upsilon(\vec{r})} \cong \frac{(\varepsilon_L + \varepsilon_H)}{2} \quad 1$$

$$\eta = \frac{1}{2}\left(\frac{\partial^2 E}{\partial N^2}\right)_{\upsilon(\vec{r})} \cong \frac{(\varepsilon_L - \varepsilon_H)}{2} \quad 2$$

$$S = \frac{1}{\eta} \quad 3$$

$$\omega = \frac{\mu^2}{2\eta} \quad 4$$

2.8. Bioplastic Production

Chitosan is combined with a plasticiser, including a mixture of glycerol, deionised water, a natural polymer such as corn starch, and 6% vinegar. The proportions of starch to chitosan and the glycerol content (20% w/v) are modified to regulate the end product's flexibility and strength. The produced liquid was agitated briskly until chitosan dissolved, facilitating the gelling process. Upon the onset of gelling, the liquid was subsequently heated to 65 °C while being stirred until it achieved transparency with the presence of bubbles. The liquid was subsequently removed from the heater and applied as a thick film onto the mould. Subsequently, it was allowed to solidify entirely for 2-3 days [26].

3. Results

The primary objective of this project was to isolate biopolymers from marine bioresources and waste materials sourced from species like crabs and periwinkles, with the goal of developing a biodegradable plastic product at the end. This research identifies suitable extraction methods for chitin and chitosan as a crucial phase in bioplastic production. The specimens employed were derived from crab shells and periwinkle shells. Chitosan is obtained from crab and periwinkle shells using procedures such as deproteinisation, demineralisation, decolouration, and deacetylation. A thorough investigation was conducted to determine the characteristics of the extracted material using FTIR spectroscopy, energy dispersive spectroscopy (EDS), scanning electron microscopy (SEM), and X-ray dispersive analysis. Figure 2 illustrates a simplified process for extracting chitosan from crustacean exoskeletons (shells).

3.1. Fourier Transform Infrared Spectroscopy (FTIR) for Periwinkle and Crab

The analytical results obtained from FTIR spectroscopy, as shown in Figure 3 regarding the extraction of chitosan from periwinkle and crab shell, establish the functional groups present in the chitosan molecular structure. FTIR spectroscopy results indicated the presence of functional groups such as hydroxyl (O-H), amine (N-H), and carbonyl (C=O) in periwinkle and crab chitosan samples. These groups are essential for adsorption as they enhance surface interaction capabilities. The O-H stretching vibration observed in periwinkle chitosan at 3691 cm^{-1} and in crab chitosan at 3457 cm^{-1} indicates structural variations attributable to the sources of extraction. The periwinkle shell exhibited peaks corresponding to the primary functional groups: N-H (amines) at 3442 cm^{-1}, O-H (hydroxyl) at 3691 cm^{-1}, and -COO (esters) at 3671.41 cm^{-1} and 1798.72 cm^{-1}, respectively. This

 doi:10.20944/preprints202603.1425.v1

finding aligns with previous research by Aimikhe et al. [13], who identified ten peaks in their FTIR analysis of periwinkle shells. Their research highlighted the peak intensities and functional groups in the chitosan extracted from the periwinkle shell. The ChC peaks associated with the major functional groups were identified at 3475 cm^{-1} for N-H (amines), 1712 cm^{-1} for O-H (hydroxyl), and 1275 cm^{-1} for aldehyde and –COO (esters). The findings are consistent with previous investigations by Mulyati et al. [27] and Odili et al. [28]. The prominent functionalities in both ChC and ChP indicate the retention of the Ch structural backbone, even after undergoing various chemical treatments. The summaries of the observed bands in the FTIR spectrum of ChC and ChP are illustrated in Table 1. The amine group acts as an electron donor and chelating site, enhancing interactions with other chemical species and adsorption characteristics. This phenomenon will be further illustrated through quantum mechanical studies in the subsequent section. The chemical structure of an adsorbent is primarily defined by the functional groups present on its surface, which significantly influence the adsorption process. The ionic interactions and extensive intermolecular hydrogen bonding among the -NH_2 groups of chitosan facilitate polymer linkage, leading to the formation of long-chain biomolecules and consequently enhancing the mechanical properties in both aquatic organisms. This result confirms the successful isolation of chitosan from the ChC and ChP shells.

Table 1. The FTIR bands assignment for ChC, ChP and their comparison to similar materials in the literature.

Functional group/vibrational modes	ChC (cm^{-1})	ChP (cm^{-1})	Lit [26]
O-H stretch overlapped with N-H stretch and inter-hydrogen bonds of the polysaccharide	3452	3428	3356
C-H stretch	2925	2931	2921
υ (C-H) in the pyranose ring	-	2867	2871
υ (C=O) in $NHCOCH_3$ group (Amide I band)	2054	1802	1652
δ (CH_2) in CH_2OH group	1446	1431	1420
υs (C-O-C) (glycosidic linkage)	1138	1051	1149
δ Pyranose ring skeletal vibrations	865	878	892

3.2. X-Ray Diffraction (XRD) of Periwinkle and Crab

XRD examination was conducted on the ChC and ChP materials derived from crustacean shells. This investigation aimed to examine the crystal orientation and structure of chitosan from various sources, together with the functional features of the organic matrix components that significantly influence the physical and biological characteristics of the resultant chitosan materials. The XRD patterns of chitosan derived from crab and periwinkle shells are illustrated in Figure 4. Figure 4 illustrates that ChC and ChP chitosan samples display two distinct strong diffraction peaks at 19.80° and 42.50°. The peaks in the XRD patterns of chitosan materials from both sources were analogous to those of other previously documented crustacean species [29,30]. The XRD diffractogram revealed semi-crystalline structures in both chitosan sources, essential for mechanical strength and flexibility. The amorphous characteristics of processed chitosan are evidenced by the broad expanded peak and elevated intensities, which increase the surface area for adsorption applications. Kusumaningrum et al. [14] emphasised analogous results in the fabrication of biodegradable plastics utilising prawn shell chitosan, whereby structural changes enhanced flexibility and adsorption characteristics. This may also explain the reduced rigidity of the crab shell in comparison to the periwinkle, characterised by a pronounced and high-intensity peak.

 doi:10.20944/preprints202603.1425.v1

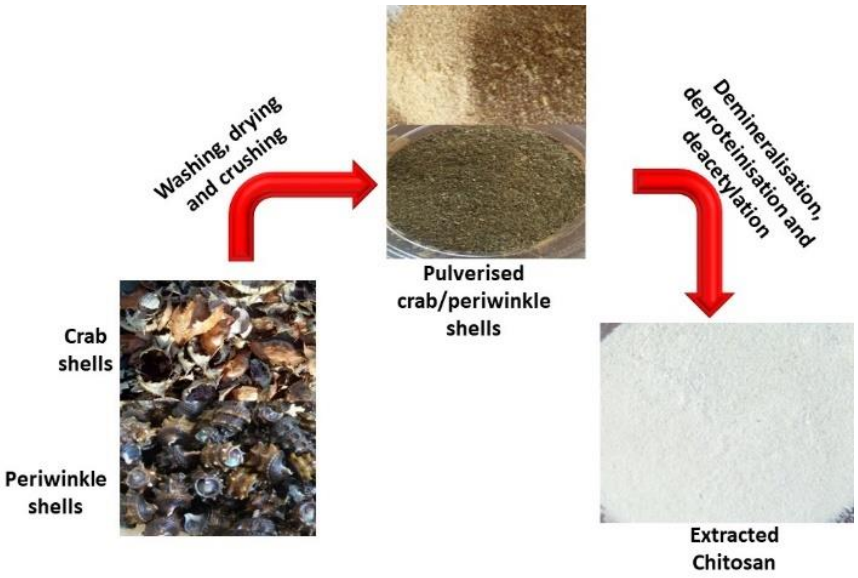

Figure 2. A simplified scheme for chitosan extraction from crustacean shells.

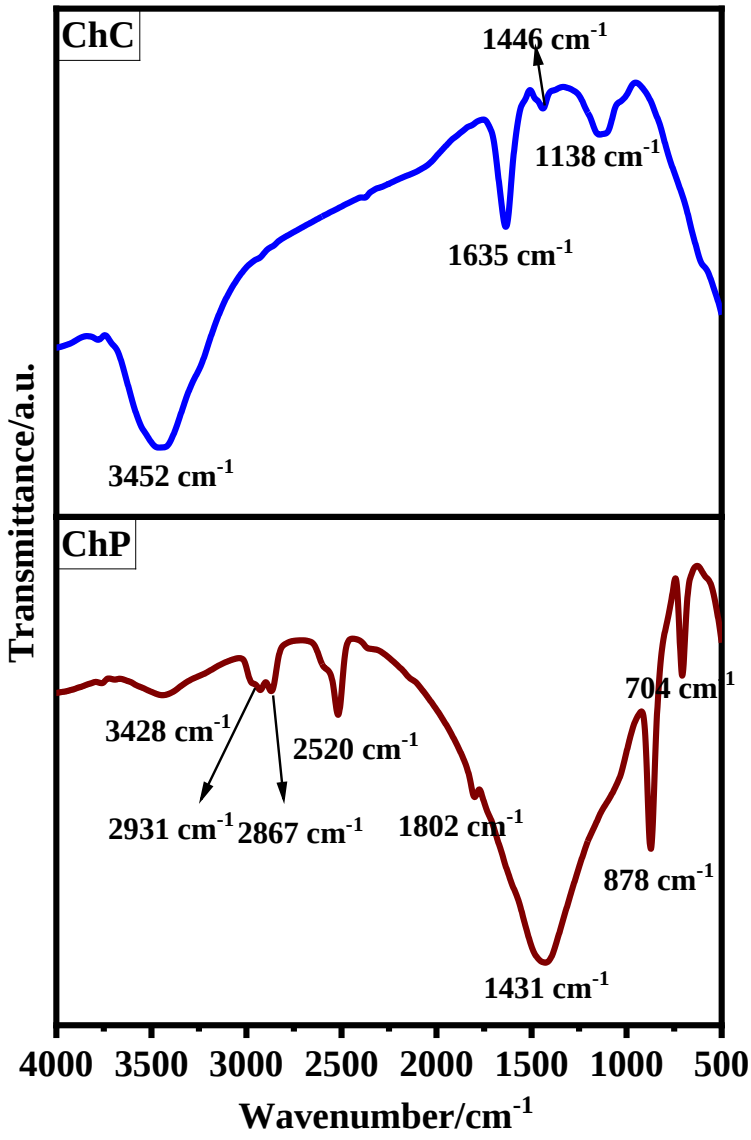

Figure 3. FTIR spectra for chitosan extracted from crab (ChC) and periwinkle (ChP) shells.

 doi:10.20944/preprints202603.1425.v1

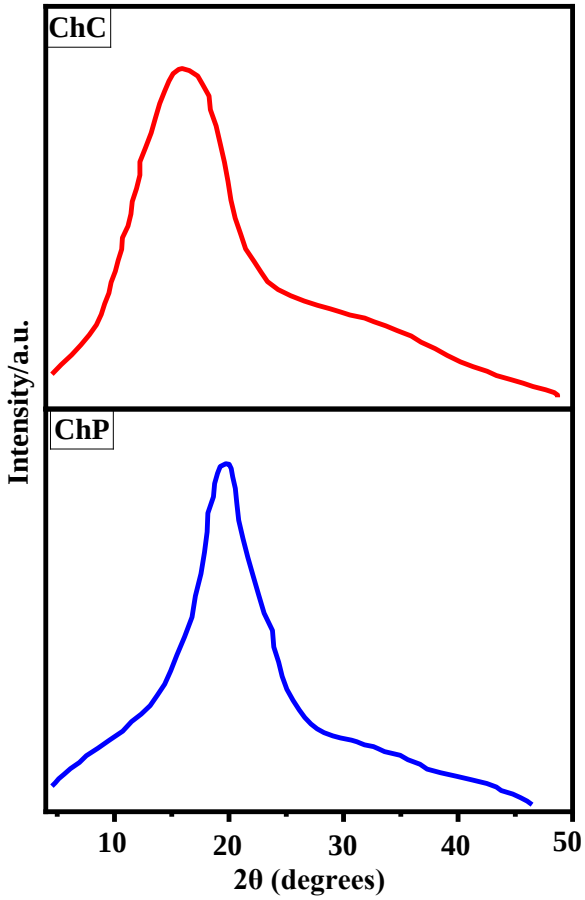

Figure 4. XRD pattern of the obtained chitosan from crab (ChC) and periwinkle (ChP).

3.3. Morphological Studies of ChC and ChP

SEM micrograph depicting the surface morphology of ChC and ChP materials derived from the two sources (Figures 5a and b). The surface morphology of the material from both sources is unique, exhibiting partial similarity in surface appearance. ChC (Figure 5a) was seen to consist of smooth, uniform scaly layers, including well-dispersed, consistently formed microfibrous structures on its surface. This is denoted by the short yellow arrows and circles, respectively. This morphology may account for the smooth surface and elevated porosity found in the crab shells and the resultant powdered chitosan (inset images, Figure 5a). Consequently, this may elucidate the cause of the crab shell's brittleness, independent of other circumstances. In contrast, the surface morphology of ChP (Figure 5b) displays uneven ripples and scaly layers, along with rough, irregularly formed microfibrous structures, as illustrated by the short red arrows and circles. This characteristic may account for the elevated mechanical strength and hardness noted in periwinkle shells, as well as the coarseness detected in the chitosan powder (inset images, Figure 5b). The variation in their morphological structure may account for the quality of the bioplastic produced from the moulding experiment, as will be discussed in a subsequent section. Both chitosan sources have a resemblance in the presence of ripple-like layers and microfibrillar structures. Uğurlu [29] indicated that the surface morphology of chitosan derived from *P. caerulea* shells has a rough, porous, fibrillar, and nano-fibril structure. The chitosan materials derived from M. turbinata shells exhibited a thick, porous, lamellated, and fibrillar structure. Bernabe et al. [31], in their investigation of the antifungal resistance of chitosan derived from the shells of the freshwater Chilean crab (Aegla chilensis) using various acid techniques, they observed that the surface shape of chitin was non-porous and rough. The present work corroborates earlier research, confirming the precision of the generated chitosan materials.

 doi:10.20944/preprints202603.1425.v1

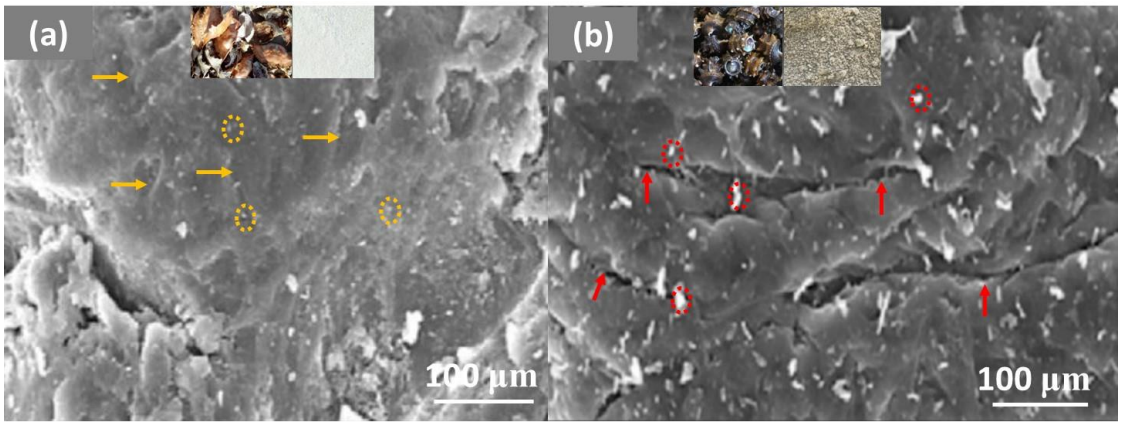

Figure 5. (a) SEM micrograph of chitosan from (a) crab and (b) periwinkle shell samples.

3.4. Energy Dispersive Spectrum of Periwinkle and Crab

Figure 6a and b illustrate the EDX spectrum of ChC and ChP materials. The EDX spectra (Figure 6a) indicated that ChC is composed of the following elements with their respective elemental compositions in percentages: Calcium (Ca; 50.60%), Magnesium (Mg; 2.70%), Carbon (C; 5.00%), Oxygen (O; 25.00%), Silicon (Si; 2.21%), Phosphorus (P; 10.00%), Sodium (Na; 2.42%), and Sulphur (S; 2.15%). Calcium is regarded as the most abundant element in crab, followed by oxygen. The presence of carbon (C) and oxygen (O) indicates the potential for organic compounds or carbonates. Other elements, including Mg, Si, P, Na, and S, are present in trace amounts. This finding aligns with the work of Olafadehan et al. [32], which indicates that the EDS spectrum shows the largest peaks for calcium, oxygen, and magnesium, while sulphur, phosphorus, and magnesium exhibit relatively low peaks, suggesting their trace levels in crab shell wastes. In contrast, the ChP EDX spectrum (Figure 6b) exhibits a significantly higher elemental composition than that of the ChC. The elemental composition observed in ChP, along with their respective percentages, includes Calcium (Ca; 54.60%), Magnesium (Mg; 3.60%), Carbon (C; 4.0%), Potassium (K; 0.10%), Oxygen (O; 20.0%), Silicon (Si; 0.01%), Phosphorus (P; 17.0%), Sodium (Na; 0.02%), and Sulphur (S; 0.02%) (Figure 6b). The analysis indicated that the predominant element in ChP is calcium, followed by oxygen. Our findings align with the report by Odili et al. [28], which indicated that calcium-related compounds constitute the majority of the material examined. Owamah et al. [33] reported that the X-ray fluorescent (XRF) spectroscopic analysis of the periwinkle shell indicates that it is primarily composed of calcium oxide, with a concentration exceeding 90%. This percentage significantly exceeds that of crab, elucidating the rationale for the superior mechanical strength and structure observed in the periwinkle shell. Zhan et al. [34] and Kusumaningrum et al. [14] emphasise the critical importance of chitosan in sustainable product development. The conversion of seafood waste into biomaterials for diverse applications, such as bioplastics, aligns with the present study's investigation of chitosan for environmental sustainability. Kusumaningrum et al. [14] advocate for integrating marine-derived biopolymers in the development of eco-friendly materials, highlighting their superior mechanical and biodegradable properties. The findings indicate the potential of periwinkle and crab chitosan for sustainable applications, including water treatment and bioplastic production. The morphological and chemical properties identified in this study indicate possible routes for adapting chitosan modifications to satisfy various industrial requirements.

 doi:10.20944/preprints202603.1425.v1

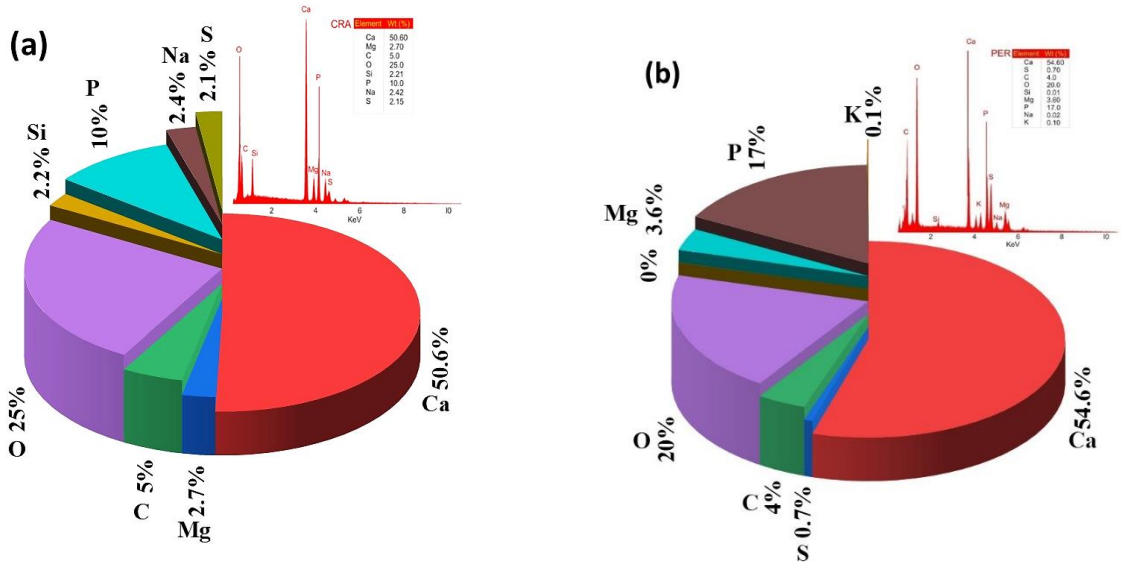

Figure 6. EDX Spectra of (a) ChC and (b) ChP shell.

4. DFT Studies of Chitosan Physicochemical Properties

Figure 7 presents the optimised configurations for the studied chitosan (Ch). The optimised structure of Ch (Figure 7) shows an average C-C bond length of 1.52 Å. The bond lengths of C-O and C-N in pyranose were measured at 1.44 Å and 1.45 Å, respectively. The quantum chemical data used to clarify the physicochemical properties and compare with experimental results pertain solely to the compound's lowest-energy conformer under investigation. The frontier molecular orbital theory posits that the interactions between the HOMO and LUMO of interacting species significantly influence chemical reactivity [35]. Furthermore, various quantum chemical parameters were calculated to enhance the understanding of intermolecular interactions and optoelectronic properties associated with Ch.

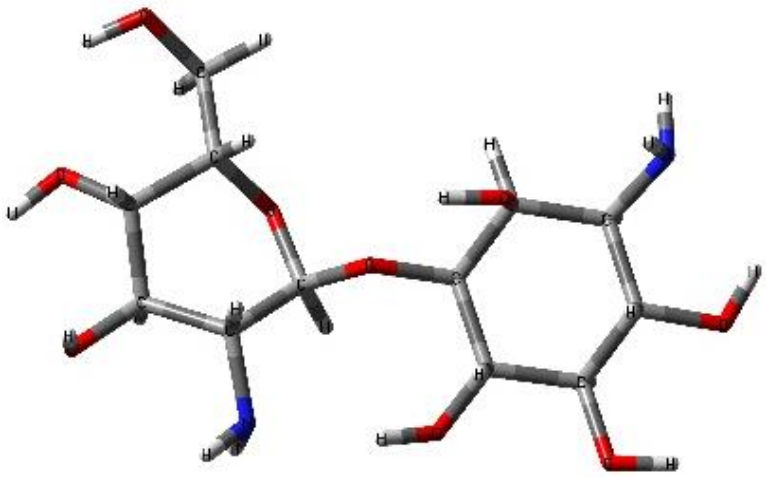

Figure 7. Optimised chitosan molecule from DFT calculation.

4.1. Molecular Vibrational Frequency

Figure 8 illustrates the simulated theoretical vibrational frequency and functions as a reference for comparison with the associated experimental FTIR spectrum of the extracted Ch. The theoretical peaks were produced using an appropriate Gaussian broadening with a half-width at half-height (HWHH) of 8 cm^{-1}. The amide I band was detected at 1654 cm^{-1} in the experimental spectra for ChC and at 1802 cm^{-1} in the spectrum for ChP. The identified distinctive bands were contrasted with the

 doi:10.20944/preprints202603.1425.v1

findings of Dreve et al. [36] about the hydrogel samples of Ch. These bands hold prominent significance in the analysed systems, and precise identification of their origin can be substantially aided by theoretical computing. Our simulation of the Ch dimer in a vacuum indicates a peak at wavenumbers between 1670 and 1505 cm^{-1}. These modes are exclusively linked to N-H bending in primary amides, with negligible contribution from C-N stretching; hence, we attribute them to the amide II band. The vibrational modes identified in the theoretical calculations are compared with the experimental results, and the summary is shown in Table 2.

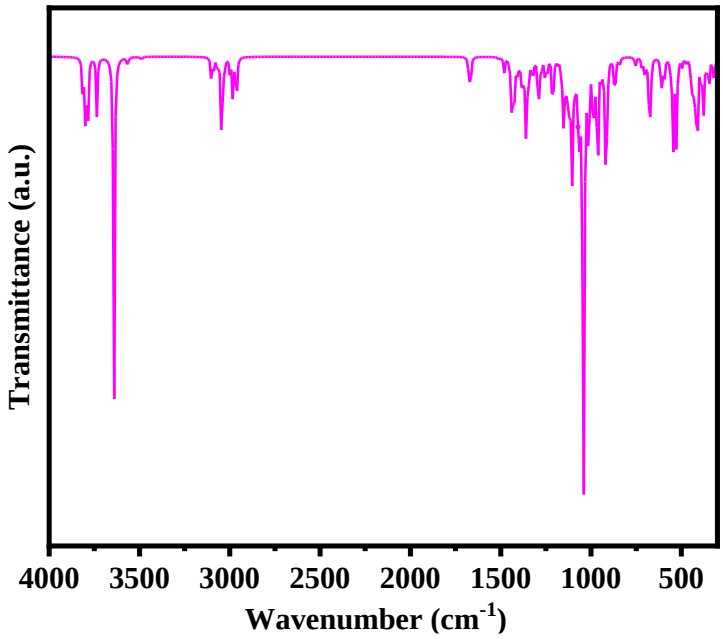

Figure 8. Theoretical vibrational frequency spectrum for optimised chitosan molecule.

Table 2. Comparison of experimental and theoretical vibrational frequency assignment.

Functional group/vibrational modes	ChC (cm^{-1})	ChP (cm^{-1})	Cal (cm^{-1})
O-H stretch overlapped with N-H stretch and inter-hydrogen bonds of the polysaccharide	3452	3428	3640
C-H stretch	2925	2931	3045
υ (C-H) in pyranose ring	-	2867	2991
υ (C=O) in $NHCOCH_3$ group (Amide I band)	2054	1802	-
δ (CH_2) in CH_2OH group	1446	1431	1430
υs (C-O-C) (glycosidic linkage)	1138	1051	1155
δ Pyranose ring skeletal vibrations	865	878	909

4.2. Optoelectronic Spectroscopy

Theoretical calculations of the optoelectronic properties of Ch were conducted to identify its critical absorption bands and the excited states of the molecule. The analysis utilised the TD-DFT/B3LYP method with a 6-311++G(d, p) basis set in a vacuum environment (Figure 9). Due to the challenges associated with directly measuring its UV-visible spectrum, utilising this theoretical approach represents the most efficient meth-od for investigating the optical properties of these polymers. The simulation predicted a significant electronic absorption peak, with a notable singlet excitation at a wave-length of 189 nm. The results highlight the influence of the contributing orbital on the observed spectrum.

 doi:10.20944/preprints202603.1425.v1

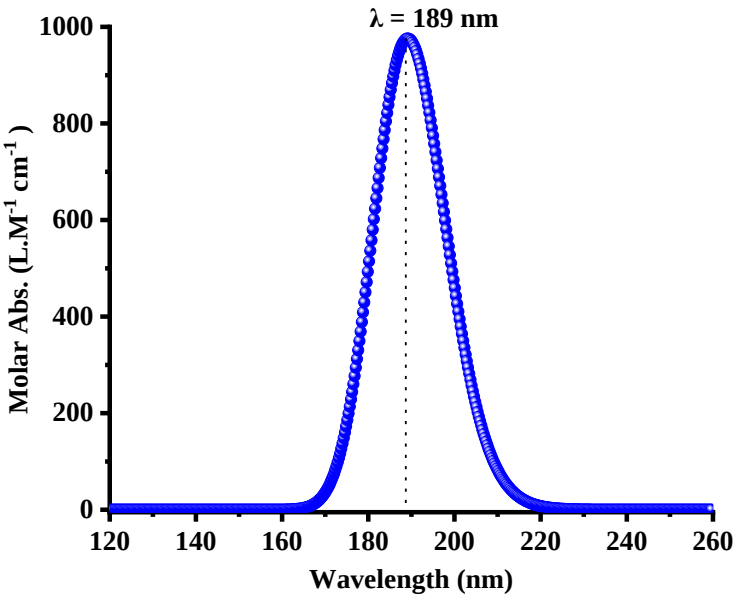

Figure 9. Theoretical UV-vis spectrum for optimised chitosan molecule.

4.3. Frontier Molecular Orbital Analysis

The energies of molecular orbitals, particularly the HOMO and LUMO, provide essential insights into the reactivity of chemical species. They illustrate the spatial arrangement of orbitals within the molecule. The orbitals are predominantly uniformly arranged around a single pyranose ring in the Ch dimer. The E_{HOMO} is typically associated with the molecule's electron-donating ability. An elevated E_{HOMO} value indicates a stronger propensity of the compound to donate electrons to an appropriate recipient species with low energy and vacant or partially filled atomic or molecular orbitals. Table 3 illustrates evidence indicating that Ch possesses a substantial E_{HOMO} value, implying a pronounced propensity for Ch to donate electrons. The compound's pronounced electron-donating capacity is ascribed to the presence of substituents with -NH groups, which facilitate electronic charge transfer to the system. Nonetheless, the -O-H group exhibits electron-withdrawing characteristics. As a result, the Ch molecule possesses a dipole.

The transition of an electron from the HOMO to the LUMO signifies the absorption of electronic energy as it moves from the lowest energy state to the first higher energy level. Elevated first and second hyperpolarizability levels, which measure the nonlinear optical (NLO) activity of a molecular system, are associated with the displacement of electron clouds from donor to acceptor groups by intermolecular charge transfer. The HOMO is primarily located near the amide group, whereas the LUMO is predominantly localised near the amine-methylene moiety. This indicates that charge transfer transpires from the amide group to the amine-methylene moiety through the hydrogen bond, which is essential for attaining a substantial second-order nonlinear optical (NLO) response. The optical gap is defined as the difference between the LUMO energy of 0.001 eV and the HOMO energy of -0.252 eV, resulting in a gap of -0.251 eV. The electrical configuration of the HOMO and LUMO energy levels is seen in Figure 10. The measured electronic characteristics of Ch indicate its possible application as an adsorption material. This is due to its ability to readily establish an electrostatic bond with the analyte. The reasoning is additionally corroborated by the electronegativity values (X) of the compounds, as presented in Table 3. Global reactivity descriptors are utilised to forecast trends in global reactivity. Utilising Koopmans' theorem and Eqs. 1-4, we calculated various parameters, including chemical hardness, electron affinity, electronic chemical potential, chemical softness, global electrophilicity index, and ionisation potential, denoted as (η, A, μ, S, ω, and I), respectively [37,38]. The frontier molecular energy gap is crucial for evaluating a molecule's chemical reactivity and stability. The relationship between chemical hardness and softness values suggests advantageous kinetic stability, consistent with computed chemical hardness values and

 doi:10.20944/preprints202603.1425.v1

demonstrating a balance between reactivity and stability. An inclination for electrophilic interactions, as evidenced by the electrophilicity index derived from DFT simulations, has been observed experimentally in reactions involving analogous polymer derivatives [39]. Compared to the previously published study [40], the results shown in Table 3 indicate that the Ch polymer has enhanced kinetic stability.

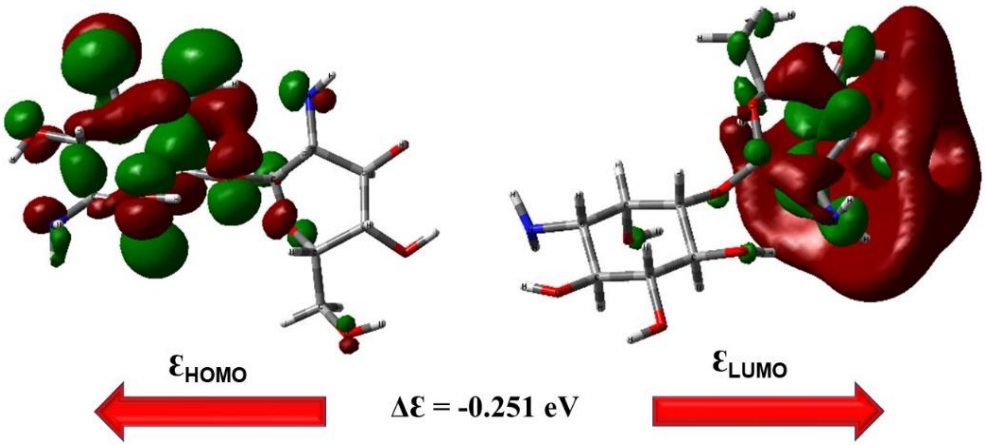

Figure 10. HOMO-LUMO energy plot and bandgap energy of the Ch molecule.

Table 3. Summary of the estimated chemical reactivity descriptors for Ch molecules.

Molecular orbital energies and Quantum chemical properties	Estimated Values (eV)
ε_{HOMO}	-0.252
ε_{LUMO}	0.001
Energy gap; $\Delta\varepsilon = \varepsilon_{LUMO} - \varepsilon_{HOMO}$	-0.251
Global electrophilicity Index (ω)	0.062
Electronic chemical potential (μ)	-0.126
Chemical Softness (S)	7.930
Global Hardness (η)	0.126
Ionisation Energy (I)	0.001
Electron affinity (A)	-0.252

4.4. Electrostatic Surface Potential (ESP) Mapping

Figure 11 (a) depicts the electrostatic potential (ESP) for Ch, offering an effective means to represent the properties and behaviour of atoms and molecules relating to their charge distribution. The data is represented on a surface exhibiting uniform electron density. The ESP was employed to determine the chemical reactivity of sites and the polarity of the Ch molecule, as demonstrated by a dipole moment of 4.0898 Debye, which may be challenging to ascertain using traditional analytical methods. The ESP calculation aids in predicting locations susceptible to electrophilic and nucleophilic attacks [41]. The different colours on the ESP mapping represent specific electrostatic potential levels. The regions shown in red, blue, yellow, and green represent the maximum degrees of electrophilic reactivity, nucleophilic reactivity, and zero electrostatic potential, respectively. The potential diminishes in the following sequence: blue > green > yellow > orange > red. The positive charge is predominantly localised around the nitrogen atom of the amine group, rendering it an advantageous site for electrophilic assault. This observation is corroborated by the electronic contour lines of charge depicted in Figure 11 (b). A low potential red area indicates an abundance of electrons. The active sites of Ch, as illustrated in Figure 11 (b), are the NH_2 functional groups. The observation suggests that charge delocalisation in the Ch molecule is governed by the interaction between electron-rich regions and electron-deficient areas of the molecule. This contact enables the

 doi:10.20944/preprints202603.1425.v1

transit of carriers within the polymer. Figure 11 (c) illustrates the amalgamation of the ESP and contour lines to enhance understanding of the electronic distribution throughout the molecule. The plots indicate that Ch possesses considerable capacity for electronic interaction and polarisability with other molecules when utilised as an adsorbent material.

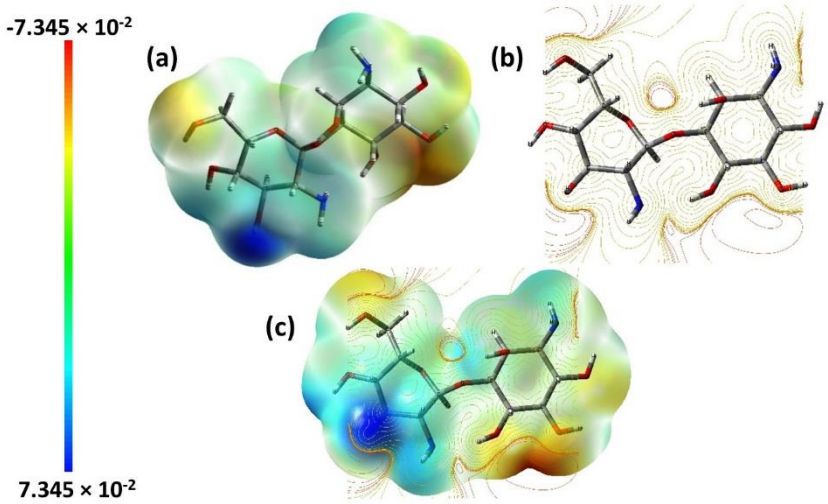

Figure 11. (a) ESP mapping, (b) Contour mapping and (c) combined ESP and contour mapping of the Ch molecule.

4.5. Chitosan Applications in Bioplastic Production

Bioplastics were effectively produced utilising ChC and ChP obtained from crustacean shell waste. The process encompassed multiple stages, such as demineralisation and deproteinisation of the shells to extract chitin, subsequently converting it to chitosan via an alkaline treatment. Chitosan was blended with glycerol as a plasticiser and corn starch to create a bio-friendly polymer matrix. The mixture was dissolved in a suitable solvent, gelled, and shaped into an environmentally friendly bioplastic product, as shown in Figure 12 (a and b). The moulded components were dried to create a solid bioplastic. Prior research has investigated the creation of environmentally sustainable and biodegradable bioplastics utilising chitosan derived from crab shells and starch sourced from rice [16,42]. Chitosan bioplastics, sourced from chitin in crustacean shells, exhibit potential applications across various sectors, including packaging, healthcare, environmental remediation, and food industries [43]. The moulded bioplastic product depicted in Figure 12 (a) does not appear to form correctly. Conversely, this is not the case for the bioplastic derived from ChP. This notable difference can be ascribed to the morphological and design variations in their shells. This structural difference has been previously elucidated in sections 3.3-3.4. With minor modifications or the integration of suitable additives, the bioplastic depicted in Figure 12 (b) can be enhanced further. These results indicate the potential use of chitosan derived from crustaceans as a sustainable material for bioplastic production and various applications.

 doi:10.20944/preprints202603.1425.v1

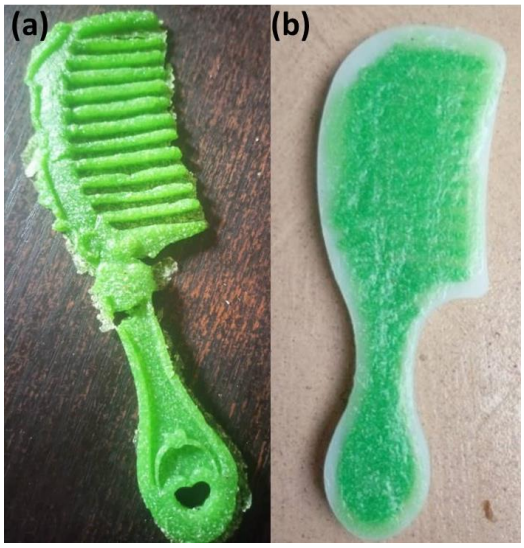

Figure 12. Moulded Bioplastic from (a) ChC and (b) ChP polymers.

5. Conclusions

This paper offers a comprehensive experimental and computational analysis of the transformation of seafood shell waste into chitosan-based bioplastics. Chitosan was effectively recovered from the shells of *Callinectes pallidus* (crab) and *Thais coronata* (periwinkle), and its capacity to make bioplastics was confirmed by blending it with starch and glycerol. FTIR spectra validated the preservation of essential functional groups (O-H, N-H, and C-O), whilst XRD analysis revealed a semi-crystalline structure characterised by distinct sharp and broad peaks. SEM pictures demonstrated a coarse, fibrous texture conducive to film formation, while EDS analysis indicated that periwinkle-derived chitosan possessed elevated carbon (38.76%) and oxygen (53.17%) content, rendering it more appropriate for flexible polymer applications compared to crab-derived chitosan. Theoretical research using DFT corroborated these experimental results. The computed HOMO-LUMO energy gap of -0.251 eV affirmed the chemical stability of chitosan, although a dipole moment of 4.0898 Debye indicated robust intermolecular interactions. Theoretical vibrational spectra aligned with the experimental FTIR measurements, confirming the chemical identification of the biopolymer. These data collectively indicate that chitosan produced from periwinkle is a strong candidate for bioplastic production due to its advantageous elemental composition and shape. The alignment of experimental findings and quantum chemical modelling substantiates the methodology and offers a scalable pathway for marine waste valorisation. This study provides essential insights into the design of biodegradable materials within a circular economy framework, in accordance with global sustainability objectives and the progression of green materials science. Although the achievement of large-scale production and international commercialisation of bioplastic products requires more research. Conclusively, this study underscores the structural and functional distinctions between periwinkle and crab chitosan, reinforcing their potential as versatile biomaterials.

Author Contributions: For research articles with several authors, a short paragraph specifying their individual contributions must be provided. The following statements should be used "Conceptualization, IOE.; methodology, ONA, AAA, JNS, MA and JA.; software, HOS and MS.; validation, HOS, IOE. and AG.; formal analysis, X.X.; investigation, X.X.; resources, X.X.; data curation, ONA, HOS, AG; writing-original draft preparation, JA, AAA, JNS.; writing—review and editing, IOE, HOS, and ONA; supervision, IOE and OPN.; project administration, IOE and OPN.; funding acquisition, JA, AAA, JNS, MA and HOS. All authors have read and agreed to the published version of the manuscript.".

 doi:10.20944/preprints202603.1425.v1

Funding: This research is partly funded by the Authors from Lagos State University, Ojo Campus and the Walter Sisulu University Research Office, Mthatha.

Data Availability Statement: All data generated and analysed during this study are included in this article.

Acknowledgments: Sincere appreciation and gratitude to the entire staff members of the Department of Fisheries and Chemistry of Lagos State University, Lagos, Nigeria. HOS and MS are grateful to Walter Sisulu University for providing computational resources and postdoctoral funding.

Conflicts of Interest: The authors declare that they have no competing interests.

References

1. Hedlund, J. The Development of Plastics in the United States: A Political Economic, Hist. Soc. Anal. 2023: North Carolina State University.
2. Marsh, K; Bugusu, B. Food packaging-roles, materials, and environmental issues, J. Food Sci. 72 (2007) R39-R55. 10.1111/j.1750-3841.2007.00301.x
3. Tamošaitienė, J.; Parham, S.; Sarvari, H.; Chan D. W.; Edwards, D. J. A review of the application of synthetic and natural polymers as construction and building materials for achieving sustainable construction, Buildings. 14 (2024) 2569. https://doi.org/10.3390/buildings14082569
4. Kjärstad, J. F. Johnsson, Resources and future supply of oil, Energy policy. 37 (2009) 441-464. https://doi.org/10.1016/j.enpol.2008.09.056
5. Baytekin, B., H.T. Baytekin, B.A. Grzybowski, Retrieving and converting energy from polymers: deployable technologies and emerging concepts, Ener. Env. Sci. 6 (2013) 3467-3482. https://doi.org/10.1039/C3EE41360H
6. Hayes, G., M. Laurel, D. MacKinnon, T. Zhao, H.A. Houck, C.R. Becer, Polymers without petrochemicals: sustainable routes to conventional monomers, Chem. Rev. 123 (2022) 2609-2734. https://doi.org/10.1021/acs.chemrev.2c00354
7. Andrady, A.L. ,N. Rajapakse, Additives and chemicals in plastics, in Hazardous chemicals associated with plastics in the marine environment. 2017, Springer. p. 1-17. https://doi.org/10.1007/698_2016_124
8. Song, J.H., R.J. Murphy, R. Narayan, G. Davies, Biodegradable and compostable alternatives to conventional plastics, Phil. Trans. Royal Soc. B: Biol. Sci. 364 (2009) 2127-2139. https://doi.org/10.1098/rstb.2008.0289
9. Gadaleta, G., S. De Gisi, F. Todaro, M. Notarnicola, Carbon footprint and total cost evaluation of different bio-plastics waste treatment strategies, Clean Technol. 4 (2022) 570-583. https://doi.org/10.3390/cleantechnol4020035
10. Somanathan, A., N. Mathew, A.M. Pillai, P. Mondal, T. Arfin, Bioplastics for clean environment, in Bioplas. Sust. 2024, Elsevier. p. 313-354. https://doi.org/10.1016/B978-0-323-95199-9.00009-3
11. Bashir, K., K. Jan, S. Jan, A.L. Khan, D.J. McClements, Biodegradable and Edible Food Packaging: Trend. Tech. 2024: Elsevier.
12. Costa, A., T. Encarnação, R. Tavares, T. Todo Bom, A. Mateus, Bioplastics: innovation for green transition, Polymers, 15 (2023) 517. https://doi.org/10.3390/polym15030517
13. Aimikhe, V. ,G. Lekia, An overview of the applications of periwinkle (Tympanotonus fuscatus) shells, Curr. J. Appl. Sci. Technol. 40 (2021) 31-58. 10.9734/CJAST/2021/v40i1831442
14. Kusumaningrum, M., H. Ardhiansyah, I.N. Pradnya, M.R.F. Putra, A.B. Fadhil. Application of Nata de Coco and Shrimp Skin Waste as a Material for Production of Biodegradable Plastic-Mini Review. in IOP Conference Series: Earth Environ. Sci. 2024. IOP Publishing. 10.1088/1755-1315/1381/1/012025
15. Liu, Y., L. Wang, L. Zhao, Y. Zhang, ZT. Li, F. Huang, Multiple hydrogen bonding driven supramolecular architectures and their biomedical applications, Chem. Soc. Rev. 53 (2024) 1592-1623. https://doi.org/10.1039/D3CS00705G
16. Duraisamy, PA, Vinod R. Extraction, characterisation, antimicrobial activity of chitosan extracted from crab shell and preparation of chitosan-based bioplastic film for food packaging, J. Adv. Sci. Res. 13 (2022) 263-268. https://doi.org/10.55218/JASR.202213130

 doi:10.20944/preprints202603.1425.v1

17. Rizeq, B.R., N.N. Younes, K. Rasool, G.K. Nasrallah, Synthesis, bioapplications, and toxicity evaluation of chitosan-based nanoparticles, Int. J. Mol. Sci. 20 (2019) 5776. https://doi.org/10.3390/ijms20225776
18. Ardean, C., C.M. Davidescu, N.S. Nemeş, A. Negrea, M. Ciopec, N. Duteanu, P. Negrea, D. Duda-Seiman, V. Musta, Factors influencing the antibacterial activity of chitosan and chitosan modified by functionalization, Int. J. Molec. Sci. 22 (2021) 7449. https://doi.org/10.3390/ijms22147449
19. Ghosh, AP.N. Jonnalgadda, Ab initio and DFT benchmark study for the calculations of isotopic shifts of fundamental frequencies for 2, 3-dihydropyran, Struct. Chem. 33 (2022) 743-755. https://doi.org/10.1007/s11224-021-01829-4
20. 2Rose, A., S.V. Kumar, S. Swavey, J. Erb, A simple and efficient protocol for screening boron-dipyrromethene dyes using TD-DFT and an examination of the aryl-meso position, Comp. Theoret. Chem. 1118 (2017) 107-114. https://doi.org/10.1016/j.comptc.2017.08.029
21. Baerends, E.J., On derivatives of the energy with respect to total electron number and orbital occupation numbers. A critique of Janak's theorem, Mol. Phys. 118 (2020) e1612955. https://doi.org/10.1080/00268976.2019.1612955
22. Musmade, N. ,L. Mahatma, Extraction and characterisation of chitosan by a simple technique from mud crabs, Intl. J. Curr. Microbiol. App. Sci. 10 (2021) 513-518. https://doi.org/10.20546/ijcmas.2021.1006.055
23. Karthick Rajan, D., K. Mohan, J. Rajarajeswaran, D. Divya, R. Kumar, S. Kandasamy, S. Zhang, A. Ramu Ganesan, β-Chitin and chitosan from waste shells of edible mollusks as a functional ingredient. Food Front. 5 (2024) 46-72. 10.1002/fft2.326
24. Al-Shamiri, H.A., M.E. Sakr, S.A. Abdel-Latif, N.A. Negm, M.T. Abou Kana, S.A. El-Daly, A.H. Elwahy, Experimental and theoretical studies of linear and non-linear optical properties of novel fused-triazine derivatives for advanced technological applications, Sci. Rep. 12 (2022) 19937. https://doi.org/10.1038/s41598-022-22311-z
25. Janak, K.E.,G. Parkin, Experimental evidence for a temperature-dependent transition between normal and inverse equilibrium isotope effects for oxidative addition of H2 to Ir (PMe2Ph)$_2$ (CO)Cl, J. Am. Chem. Soc. 125 (2003) 13219-13224. https://doi.org/10.1021/ja0362611
26. Frenchibai, P.B.B., R. Vinayagam, D. Ambigapathi, G.K. Anbazhagan, L. Elumalai, S. Palaniyandi, N. Siddan, G.S. Thangam, K. Dharmalingam, Chitosan from Shells of Crustaceans and its Application in the Synthesis of Biodegradable Polymers, Biomed. Mater. Dev. (2025) 1-10. https://doi.org/10.1007/s44174-025-00334-0
27. Handayani, I., D. Apriani, M. Mulyati, A.R.A. Zahra, N.A. Yusuf, Enhancing security and privacy of patient data in healthcare: A smartpls analysis of blockchain technology implementation, IAIC Trans. Sust. Digital Innov. (ITSDI), 5 (2023) 8-17. https://doi.org/10.34306/itsdi.v5i1.603
28. Odılı, C., O. Sekunowo, P. Gbenebour, O. Adeosun, Characterization and properties comparison of Nigerian crab-shell extracts, Usak University J. Eng. Sci. 3 (2020) 1-12. https://dergipark.org.tr/en/pub/uujes/issue/55973/739947
29. Uğurlu, E., Evaluation of gastropods as biomaterials: monodonta turbinata (Born, 1780), Acta Aq. Tur. 20 (2024) 97-107. https://doi.org/10.22392/actaquatr.1301286
30. Mohan, K., T. Muralisankar, R. Jayakumar, C. Rajeevgandhi, A study on structural comparisons of α-chitin extracted from marine crustacean shell waste, Carb. Poly. Technol. App. 2 (2021) 100037. https://doi.org/10.1016/j.carpta.2021.100037
31. Bernabe, P., L. Becherán, G. Cabrera-Barjas, A. Nesic, C. Alburquenque, C.V. Tapia, E. Taboada, J. Alderete, P. De Los Ríos, Chilean crab (Aegla cholchol) as a new source of chitin and chitosan with antifungal properties against Candida spp, Int. J. Biol. Macromol. 149 (2020) 962-975. https://doi.org/10.1016/j.ijbiomac.2020.01.126
32. Olafadehan, O.A., K.O. Amoo, T.O. Ajayi, V.E. Bello, Extraction and characterisation of chitin and chitosan from Callinectes amnicola and Penaeus notialis shell wastes, J. Chem. Eng. Mat. Sci. 12 (2021) 1-30. 10.5897/JCEMS2020.0353
33. Owamah, H., H. Uguru, L. Umukoro, O. Akpokodje, M. Helal, R. Sami, G. Alshehry, E. Algarni, N. Abdelhai, S.A. Abushal, Mechanical and Physiochemical Characteristics of Sandcrete Blocks Produced with Sustainable Biomaterials, Sci. Adv. Mat. 16 (2024) 518-531. https://doi.org/10.1166/sam.2024.4656

 doi:10.20944/preprints202603.1425.v1

34. Zhan, Z., Y. Feng, J. Zhao, M. Qiao, Q. Jin, Valorisation of seafood waste for food packaging development, Foods, 13 (2024) 2122. https://doi.org/10.3390/foods13132122
35. Obi-Egbedi, N., I. Obot, M. El-Khaiary, S. Umoren, E. Ebenso, Computational simulation and statistical analysis on the relationship between corrosion inhibition efficiency and molecular structure of some phenanthroline derivatives on mild steel surface, Int. J. Electrochem. Sci. 6 (2011) 5649-5675. https://doi.org/10.1016/S1452-3981(23)18435-5
36. Draye, J.P., B. Delaey, A. Van de Voorde, A. Van Den Bulcke, B. Bogdanov, E. Schacht, In vitro release characteristics of bioactive molecules from dextran dialdehyde cross-linked gelatin hydrogel films, Biomat. 19 (1998) 99-107. https://doi.org/10.1016/S0142-9612(97)00164-6
37. Dhonnar, S.L., N.V. Sadgir, V.A. Adole, B.S. Jagdale, Molecular structure, FT-IR spectra, MEP and HOMO-LUMO investigation of 2-(4-fluorophenyl)-5-phenyl-1, 3, 4-oxadiazole using DFT theory calculations, Adv. J. Chem.-Sec. A, 4 (2021) 220-230. 10.22034/AJCA.2021.283003.1254
38. Parr, R.G., L.v. Szentpály, S. Liu, Electrophilicity index, J. Am. Chem. Soc. 121 (1999) 1922-1924. https://doi.org/10.1021/ja983494x
39. Maleki, M., T. Tichter, G.A. El-Nagar, I. Lauermann, C. Roth, Hybrid electrospun nanofibers as electrocatalyst for vanadium redox flow batteries: theory and experiment, ChemElectroChem, 8 (2021) 218-226. https://doi.org/10.1002/celc.202001380
40. Hoque MM, Hussen MS, Kumer A, Khan MW. Synthesis of 5, 6-diaroylisoindoline-1, 3-dione and computational approaches for investigation on structural and mechanistic insights by DFT, Mol. Sim. 46 (2020) 1298-1307. https://doi.org/10.1080/08927022.2020.1811866
41. Fayemi OE, Letsholo PB, Shoyiga HO, Ahia CC, Meyer EL. Investigation of the effects of concentration and voltage on the physicochemical properties of Nylon 6 nanofiber membrane, Sci. Rep. 15 (2025) 10865-10877. https://doi.org/10.1038/s41598-025-88356-y
42. Sasria NR, Hernando M, Lubis A, Zulfikar. Production of biodegradable plastics using aking rice starch and chitosan from crab shells as a substitute for conventional plastic. in IOP Conference Series: Materials Science and Engineering. 2021. IOP Publishing. 10.1088/1757-899X/1053/1/012079
43. Bilgen HD. Chitin/Chitosan-Based Bioplastic Production from Crab Shells, New Trends in Agriculture, Forest. Aq. Sci. 179-188.